Ultrafast temporal pulse shaping via phase-sensitive three-wave mixing

Y. C. Yin,[1] **D. French,**[1] **and I. Jovanovic**[2,*]

[1]*School of Nuclear Engineering, Purdue University, West Lafayette, IN 47907, USA*
[2]*Department of Mechanical and Nuclear Engineering, The Pennsylvania State University, University Park, PA 16802, USA*

**ijovanovic@psu.edu*

Abstract: It is well-known that the process of optical parametric amplification (OPA) can be sensitive to the phases of the incident waves. In OPA realized by three-wave mixing, injection of all three waves into the same mode with appropriate phase relationship results in amplification of the signal phase, with an associated deamplification of the signal energy. Prospects for the use of this technique in the temporal domain for shaping ultrashort laser pulses are analyzed using a numerical model. Several representative pulse shaping capabilities of this technique are identified, which can significantly augment the performance of common passive pulse shaping methods operating in the Fourier domain. It is found that the use of phase-sensitive OPA shows a potential for significant compression of ~ 100 fs pulses, steepening of the rise time of ultrashort pulses, and production of pulse doublets and pulse trains. It is also shown that the group velocity mismatch can assist the shaping process. Such pulse shaping capabilities are found to be within reach of this technique in common nonlinear optical crystals pumped by pulses available from compact femtosecond chirped-pulse amplification laser systems.

OCIS codes: (320.5540) Pulse shaping; (320.5520) Pulse compression; (190.4410) Nonlinear optics, parametric processes.

References and links

1. A. M. Weiner, "Femtosecond pulse shaping using spatial light modulators," Rev. Sci. Instrum. **71,** 1929–1960 (2000).
2. A. M. Weiner, D. E. Leaird, J. S. Patel, and J. R. Wullert, "Programmable femtosecond pulse shaping by use of a multielement liquid-crystal phase modulator," Opt. Lett. **15,** 326–328 (1990).
3. M. A. Dugan, J. X. Tull, and W. S. Warren, "High-resolution acousto-optic shaping of unamplified and amplified femtosecond laser pulses," J. Opt. Soc. Am. B **14,** 2348–2358 (1997).
4. M. E. Fermann, V. da Silva, D. A. Smith, Y. Silberberg, and A. M. Weiner, "Shaping of ultrashort optical pulses by using an integrated acousto-optic tunable filter," Opt. Lett. **18,** 1505–1507 (1993).
5. P. Tournois, "Acousoto-optic programmable dispersive filter for adaptive compensation of group delay time dispersion in laser systems," Opt. Commun. **140,** 245–249 (1997).
6. F. Verluise, V. Laude, Z. Cheng, Ch. Spielmann, and P. Tournois, "Amplitude and phase control of ultrashort pulses by use of an acousto-optic programmable dispersive filter: pulse compression and shaping," Opt. Lett. **25,** 575–577 (2000).
7. R. H. Stolen and C. Lin, "Self-phase-modulation in silica optical fibers," Phys. Rev. A **17,** 1448–1453 (1978).
8. W. J. Tomlinson, R. H. Stolenn, and C.V. Shank, "Compression of optical pulses chirped by self-phase modulation in fibers," J. Opt. Soc. Am. B **1,** 139–149 (1984).
9. C. J. McKinstrie, R. O. Moore, S. Radic, and R. Jiang, "Phase-sensitive amplification of chirped optical pulses in fibers," Opt. Express **15,** 3737–3758 (2007).

#128208 - $15.00 USD Received 10 May 2010; revised 1 Jul 2010; accepted 9 Aug 2010; published 13 Aug 2010

10. X. Liu, F. O. Ilday, K. Beckwitt, and F. W. Wise, "Femtosecond nonlinear polarization evolution based on cascade quadratic nonlinearities," Opt. Lett. **25,** 1394–1396 (2000).
11. X. Liu, L. J. Qian, and F. W. Wise, "Generation of Optical Spatiotemporal Solitons," Phys. Rev. Lett. **82,** 4631–4634 (1999).
12. X. Liu, L. Qian, and F. Wise, "High-energy pulse compression by use of negative phase shifts produced by the cascade $\chi^{(2)}$:$\chi^{(2)}$ nonlinearity," Opt. Lett. **24,** 1777–1779 (1999).
13. J. Moses, E. Alhammali, J. M. Eichenholz, and F. W. Wise, "Efficient high-energy femtosecond pulse compression in quadratic media with flattop beams," Opt. Lett. **32,** 2469–2471 (2007).
14. J. Moses, B. A. Malomed, and F. W. Wise, "Self-steepening of ultrashort optical pulses without self-phase-modulation," Phys. Rev. A **76,** 021802 (2007).
15. J. Moses and F. W. Wise, "Controllable Self-Steepening of Ultrashort Pulses in Quadratic Nonlinear Media," Phys. Rev. Lett. **97,** 073903 (2006).
16. L. A. Wu, H. J. Kimble, J. L. Hall, and H. Wu, "Generation of squeezed states by parametric down conversion," Phys. Rev. Lett. **57,** 2520–2523 (1986).
17. C. M. Caves, "Quantum limits on noise in linear amplifiers," Phys. Rev. D **26,** 1817–1839 (1982).
18. G. M. D'Ariano, C. Macchiavello, N. Sterpi and H. P. Yuen, "Quantum phase amplification" Phys. Rev. A **54,** 4712–4718 (1996).
19. I. Jovanovic, D. French, J. C. Walter, and R. P. Ratowsky, "Numerical studies of multimodal phase-sensitive parametric amplification," J. Opt. Soc. Am. B **26**, 1169–1175 (2009).
20. Y. R. Shen, *The Principle of Nonlinear Optics*, (Wiley, 2003).
21. M. D. Feit and J. A. Fleck, Jr., "Computation of mode properties in optical fiber waveguides by a propagating beam method," Appl. Opt. **19,** 1154–1164 (1980).
22. M. Marangoni, C. Manzoni, R. Ramponi, and G. Cerullo, "Group-velocity control by quadratic nonlinear interactions," Opt. Lett. **31,** 534–536 (2006).
23. J. Moses and F. W. Wise, "Soliton compression in quadratic media: high-energy few-cycle pulses with a frequency-doubling crystal," Opt. Lett. **31,** 1881–1883 (2006)
24. C. Laconis and I. A. Walmsley, "Spectral phase interferometry for direct electric–field reconstruction of ultrashort optical pulses," Opt. Lett. **23,** 792–794 (1998).
25. D. Meshulach and Y. Silberberg, "Coherent quantum control of multiphoton transitions by shaped ultrashort optical pulses," Phys. Rev. A **60,** 1287–1292 (1999).
26. D. Meshulach and Y. Silberberg, "Coherent quantum control of two-photon transitions by a femtosecond laser pulse," Nature (London) **396,** 239 (1998).
27. T. Hornung, R. Meier, and M. Motzkus, "Optimal control of molecular states in a learning loop with a parameterization in frequency and time domain," Chem. Phys. Lett. **326,** 445-453 (2000).
28. R. Yano and H. Gotoh, "Tunable terahertz electromagnetic wave generation using birefringent crystal and grating pair," Jpn. J. Appl. Phys. **44,** 8470–8473 (2005).
29. X. Zhang, A. L. Lytle, T. Popmintchev, X. Zhou, H. C. Kapteyn, M. M. Murnane, and O. Cohen, "Quasi-phase-matching and quantum-path control of high-harmonic generation using counter-propagating light," Nat. Photon. **3,** 270–275 (2007).
30. I. Will and G. Klemz, "Generation of flat-top picosecond pulses by coherent pulse stacking in a multicrystal birefringent filter," Opt. Express **16,** 14922–14937 (2008).
31. M. Renard, R. Lavorel, and O. Fraucher, "Pulse trains produced by phase-modulation of ultrashort optical pulses: tailoring and characterization," Opt. Express **12,** 473–482 (2004).
32. R. A. Kaindl, M. Wurm, K. Reimann, P. Hamm, A. M. Weiner, and M. Woerner, "Generation, shaping, and characterization of intense femtosecond pulses tunable from 3 to 20 um," J. Opt. Soc. Am. B **17,** 2086–2094 (2000).

1. Introduction

With the advent of ultrashort laser pulses and their use in diverse fields such as communications, coherent control of chemical reactions, materials processing, and intense laser-matter interactions, pulse shaping has emerged as an important technique frequently integral to ultrafast applications. Pulse shaping has been used to tailor laser-matter interactions to deliver enhancements of the phenomena induced by ultrafast laser pulses. Ultrafast shaping methods demonstrated and extensively used to date are usually passive and based on the manipulation of the Fourier (spectral) domain [1], circumventing the cumbersome or unfeasible direct manipulation of the ultrafast temporal field. Various technologies for ultrafast pulse shaping have been developed, including programmable spatial light modulators [2], acousto-optic modulators [3], and acousto-optic programmable dispersive filters [4–6].

#128208 - $15.00 USD Received 10 May 2010; revised 1 Jul 2010; accepted 9 Aug 2010; published 13 Aug 2010

While the passive Fourier-domain pulse shaping method has been very successful to date in producing diverse pulse shapes required by applications, it exhibits several limitations originating from the fact that it can be considered to be an optical filter. Its principal limitation is the incapability to produce pulses with temporal features shorter than that determined by the spectral content of the original pulse. Passive pulse shaping in the Fourier domain is limited to the selective removal or relative phase adjustment of the pre-existing frequency components. This limitation can be overcome by using nonlinear pulse shaping methods which can coherently extend the frequency content of the pulse. Previously demonstrated nonlinear techniques exhibiting such capabilities include the self-phase modulation (SPM) [7, 8], phase-sensitive four-wave mixing [9], and cascaded second-order nonlinearities [10, 11]. Such nonlinear pulse shaping techniques can compress optical pulses [12, 13] and generate pulses with steep temporal features [14, 15]. Fourier representations of such pulses contain high frequencies that cannot be generated by passive Fourier domain devices.

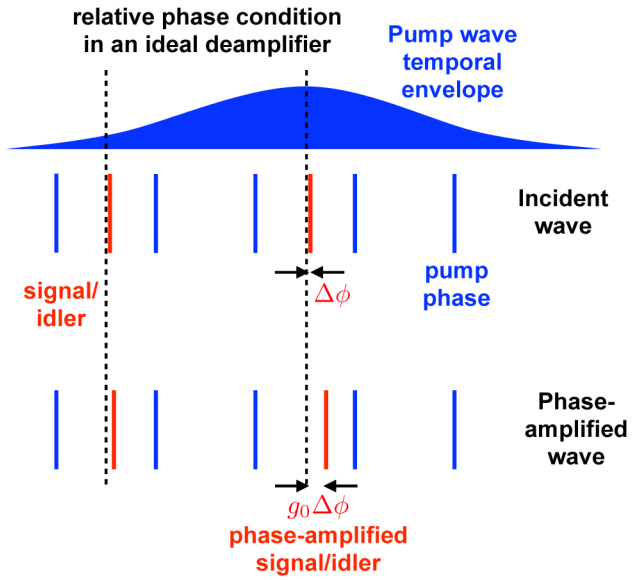

Fig. 1. Qualitative representation of the effect of temporal phase amplification on the phase of the signal/idler wave (red), shown in degenerate OPA with temporally varying pump (blue). The amplified quantity is the departure ($\Delta\phi$) of the phase difference between the signal/idler and the pump wave from the ideal power deamplification condition. The phase of the signal/idler wave is advanced or retarded at a rate dependent on the pump intensity and the original departure from the ideal power deamplification condition, with effective gain factor g_0.

In this paper, a novel method for nonlinear pulse shaping is proposed and analyzed, which directly shapes the temporal electric field amplitude and phase using the process of phase-sensitive three-wave mixing (PSTWM). PSTWM is known to produce squeezed states of electromagnetic field [16] and is typically used in the photon number amplification mode to amplify a signal without imparting additional noise [17]. An unconventional and previously unutilized mode of operation of PSTWM in the temporal domain is discussed here for the first time to the best of our knowledge. When PSTWM is operated in photon number *deamplification* mode, direct shaping of the electric field can be realized through the process of phase amplification (Fig. 1). If the small-signal deamplification gain coefficient is denoted by $g_0 : E\exp(i\varphi) \rightarrow E/\sqrt{g_0}\exp(ig_0\varphi)$ [18], where E is the amplitude of the electric field inci-

#128208 - $15.00 USD Received 10 May 2010; revised 1 Jul 2010; accepted 9 Aug 2010; published 13 Aug 2010

dent onto PSTWM, and φ corresponds to the departure of phase relationship among the pump, signal, and idler waves from the ideal deamplification condition at the input of PSTWM:

$$\varphi = \phi_3(0) - \phi_2(0) - \phi_1(0) - \pi/2, \tag{1}$$

where $\phi_1(0)$, $\phi_2(0)$, and $\phi_3(0)$ are the input phases of the signal, idler, and pump, respectively. Since this phase amplification effect is also intensity-dependent, it results in amplitude-to-phase encoding through the temporally varying gain coefficient g_0, and this aspect of the process is similar to SPM. However, the PSTWM can also broaden the spectral content of the pulse (Fig. 2), even in the case of flat pulse temporal profiles. This is possible when there is a

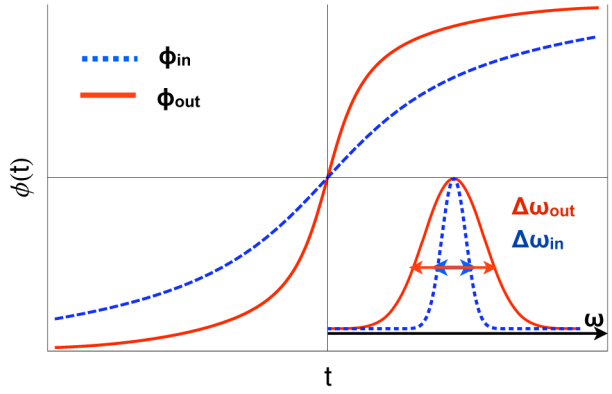

Fig. 2. Conceptual schematic of temporal phase amplification and its effect on pulse bandwidth: ϕ_{in} and ϕ_{out} are the incident and the amplified phase, and $\Delta\omega_{in}$ and $\Delta\omega_{out}$ are the incident and amplified width of the frequency spectrum, respectively. Phase amplification steepens the change of temporal phase, effectively adding spectral bandwidth to the pulse.

temporally varying phase difference among the signal, idler, and pump waves, resulting in a temporally varying departure from the ideal deamplification condition [Eq. (1)]. PSTWM is essentially a phase-sensitive cross-phase modulation process relying on $\chi^{(2)}$ nonlinearities instead of the usual $\chi^{(3)}$ nonlinearities. Unlike the previously demonstrated $\chi^{(2)}$ compression technique which uses phase-mismatched second-harmonic generation [12], our approach uses phase-matched PSTWM and is sensitive to both pulse energy and relative phase among waves. It is shown that the temporal phase amplification using PSTWM provides strong and controllable phase modulation, which can be exploited to directly generate useful pulse shape modifications, such as pulse compression, pulse steepening, pulse doublets, and pulse trains.

2. Numerical model for a plane-wave phase-sensitive OPA

A numerical model has been developed to study the effect of PSTWM on shaping ultrashort laser pulses by augmenting the previously developed model for phase amplification in the spatial domain [19]. In this study, the following assumptions and simplifications are made: (1) the mixing process is degenerate and collinear, i.e. signal and idler waves are identical, (2) the three mixing waves exist in a single spatial mode, but are longitudinally multimode, (3) the three waves experience no diffraction in the mixing process (plane waves), and (4) the nonlinear medium is lossless. The model uses standard coupled differential equations with the slowly varying envelope approximation for three-wave mixing [20], which are further simplified to coupled wave equations for second-harmonic generation since a degenerate collinear system is

#128208 - $15.00 USD Received 10 May 2010; revised 1 Jul 2010; accepted 9 Aug 2010; published 13 Aug 2010

considered:

$$\frac{dA_1}{dz} = i\frac{2d_{eff}\omega_1^2}{k_1c^2}A_2^*A_1\exp(i\Delta kz) \tag{2}$$

$$\frac{dA_2}{dz} = i\frac{d_{eff}\omega_2^2}{k_2c^2}A_1^2\exp(i\Delta kz), \tag{3}$$

where $A_{1,2}$ are the complex field amplitudes of the signal/idler (hereafter referred to as the signal) and pump waves, respectively, d_{eff} is the effective nonlinearity, ω_i is the angular frequency, k_i is the wave vector, Δk is the wave vector mismatch, and c is the speed of light in vacuum. The longitudinal coordinate is denoted by z. To address the important temporal characteristics of this process, the complex amplitude of the signal and pump pulses A_i are represented in the time and frequency domain: $A_i = A_i(t) = \mathscr{F}^{-1}[A_i(\omega)]$, including the corresponding amplitude and phase. While the coupled differential equations for the three fields are expressed and integrated in the time domain, it is also necessary to include dispersion, which is easily represented in the spectral domain. Dispersion is included in the model using the usual split-step approach [21], by transforming the fields into the spectral domain after each step of numerical integration in the time domain. The spectral phase applied to the three fields at each step is

$$A_i(\omega) \rightarrow A_i(\omega)\exp(in_i(\omega)\omega/c), \tag{4}$$

where ω is the angular frequency, and $n(\omega)$ is the refractive index for the corresponding spectral component ω of wave A_i. SPM is included in the model by applying the temporally-dependent phase to each wave

$$A_i(t) \rightarrow A_i(t)\exp(in_2^{NL}\omega_i I_i(t)dz/c), \tag{5}$$

where n_2^{NL} is the Kerr nonlinear refractive index, $I_i(t)$ is the instantaneous intensity at time t, and ω_i is the center frequency of wave A_i. The traveling frame of reference for the calculation is established in reference to the signal wave A_1 by applying the linear phase after each split step:

$$A_i(\omega) \rightarrow A_i(\omega)\exp(in_1(\omega_1)\omega_1/c), \tag{6}$$

where $n_1(\omega_1)$ is the refractive index for the signal wave at the signal center frequency ω_1. The model is solved by numerical integration in the time domain with a typical step size of $dz = 0.1\mu$m. For this study, beta-barium borate (BBO) crystal is chosen, which is known for its multiple favorable material and nonlinear properties. The incident signal beam is centered at 800 nm, while the pump is centered at 400 nm. All incident pulses are assumed to have a Gaussian spectral profile. Further, the spectral bandwidth of the three waves is chosen such that their initial transform-limited pulse duration is 100 fs. Phase matching is achieved by orienting the crystal at 29.2° from its principal axis, and the phase-sensitive deamplification condition is established by setting the initial temporal phase relationship among the three waves to $\phi_2(0) - \phi_1(0) = \pi/4$ at the peak of two pulses. It should be noted that, in principle, PSTWM can also be carried out in a nondegenerate configuration, but this study was initially restricted to the degenerate case for its simplicity and the relative ease of future experimental demonstration.

3. Temporal phase amplification without dispersion and self-phase modulation effects

In order to elucidate the principal properties of the PSTWM process resulting in temporal phase amplification, it is initially assumed that no dispersion is present and that no SPM occurs in the process. This restricts the analysis to the isolated effect of PSTWM on the temporal structure of ultrashort pulses, including the effect of phase and amplitude variation. Two characteristic examples of temporal phase amplification are considered at this point and are shown in Fig. 3. The relative phase between the incident signal and pump waves is set such that the ideal

#128208 - $15.00 USD Received 10 May 2010; revised 1 Jul 2010; accepted 9 Aug 2010; published 13 Aug 2010

deamplification condition is satisfied at the pulse center. The input temporal phase is varied by adjusting the signal phase, while keeping the pump phase constant.

In the first example, which we refer to as the quadratic case, the incident signal has a small quadratic temporal phase (chirp) with a corresponding group delay dispersion (GDD) of $\phi^{(2)} = -2091$ fs^2. In the second example, which we refer to as the linear case, the incident signal has small residual linear phase corresponding to the frequency shift $\Delta\omega = 1.47$ THz. The quadratic phase and the linear phase provide a variation in the initial phase of the signal in time, allowing for amplification of the departure of the signal phase from the ideal power deamplification condition. In both cases, the incident intensities are taken to be 5 GW/cm^2 for both input waves, and the length of the BBO crystal is chosen to be 2 mm. Results of the calculation with the dispersion and SPM turned off are shown in Fig. 3.

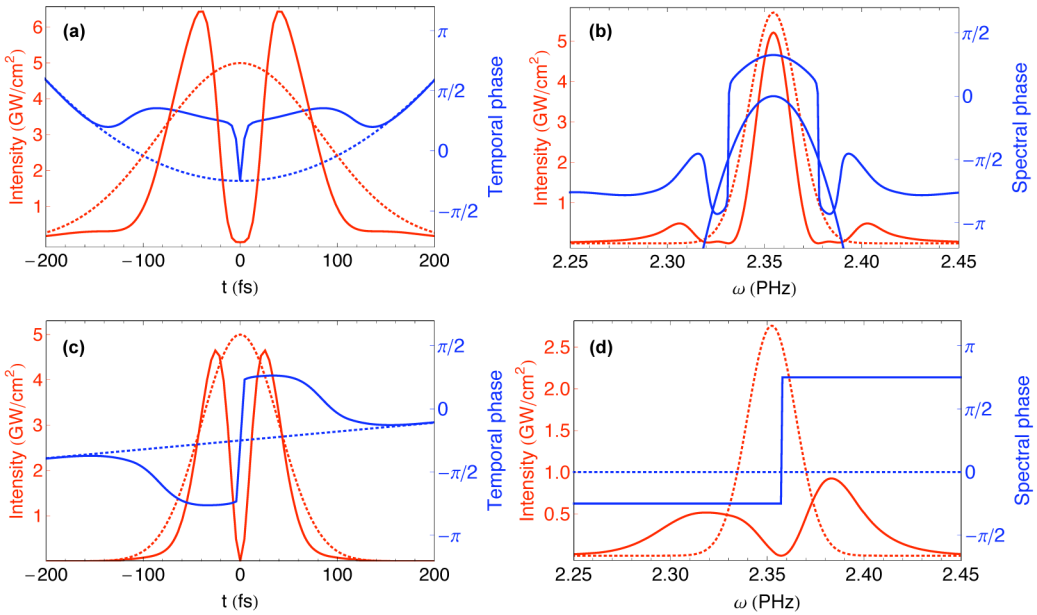

Fig. 3. Examples of temporal phase amplification with dispersion and SPM excluded from the model (input pump pulse duration: 100 fs). Shown are the temporal and spectral intensity and phase of signal/idler before (dashed) and after (solid) PSTWM. Quadratic case: (a) (Media 1) and (b); Linear case: (c) (Media 2) and (d).

In the quadratic case [Fig. 3(a) (Media 1)], temporal phase amplification and the corresponding power deamplification for the signal are clearly present. For small phase gains, the phase gain is approximately the inverse of the power deamplification gain, which indicates that in this instance PSTWM behaves similar to a single-mode quantum phase amplifier [18]. The temporal phase amplification is interpreted as the temporally varying addition (subtraction) of the electric field with phase determined by the relative phase difference between the signal and idler at that temporal point. The amplified temporal phase contributes to the additional bandwidth in the output signal. This broadening of the pulse spectral content is similar to that produced by SPM, with the difference being that the temporal phase amplification is the result of a nonlinear process governed by second-order nonlinearity $\chi^{(2)}$ rather than the third order nonlinearity $\chi^{(3)}$. The spectral broadening indicates a potential for production of shorter pulses by this method when the appropriate residual phase compensation is applied. If the phase com-

#128208 - $15.00 USD Received 10 May 2010; revised 1 Jul 2010; accepted 9 Aug 2010; published 13 Aug 2010

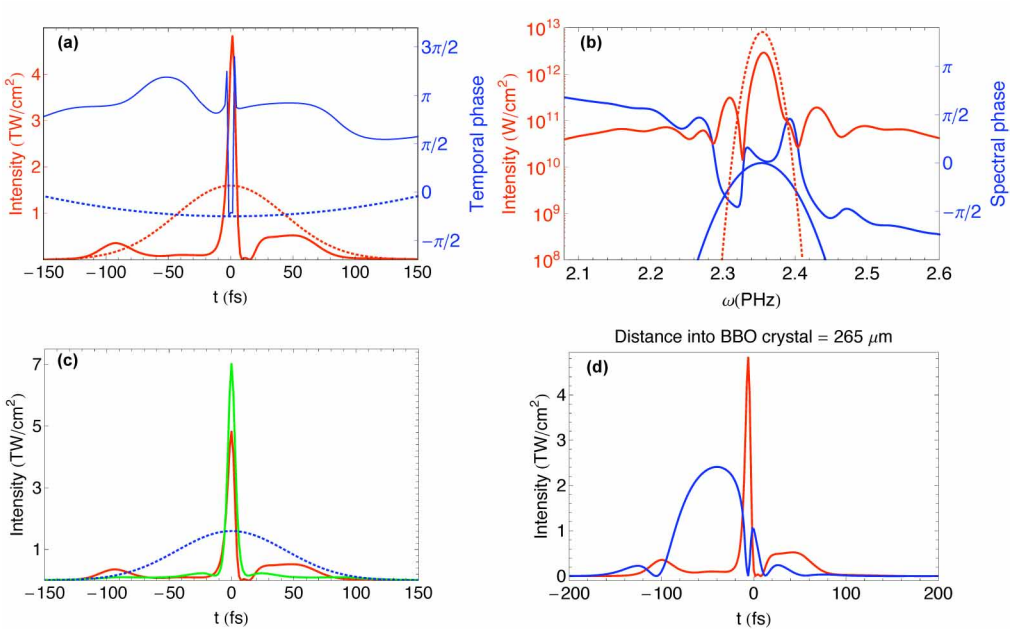

Fig. 4. Pulse compression without SPM in the quadratic case with input pump pulse duration of 100 fs: (a) Temporal intensity and phase of signal before (dashed, ∼ 100 fs) and after (solid, 6 fs) PSTWM; (b) Spectral intensity and phase of signal before (dashed) and after (solid) PSTWM; (c) Temporal intensity of signal before (blue) and after (red, 6 fs) PSTWM and output with an ideal phase compensation (green, 6 fs); (d) Pulse compression process as signal (red) and pump (blue) traverse the nonlinear medium (Media 3).

pensation is not applied, the output pulse is deeply modulated at its center as a result of more efficient power deamplification process at the pulse center. In the linear case, a similar result is obtained [Fig. 3(c) and 3(d)]. A spectral phase jump can occur in the process, as can be seen in Fig. 3(d). This is because the field at the time or frequency where the jump occurs is fully depleted. In both cases, if the additional phase compensation is applied, production of shorter pulses can be achieved. Since dispersion and SPM are neglected here, the signal and the pump are perfectly overlapped in time during the nonlinear interaction and no additional third-order phase is applied. Thus the results presented in Fig. 3 can only be considered reasonably accurate for short crystals in which the effects of group velocity dispersion are negligible and the total accumulated nonlinear phase due to the Kerr effect (B-integral) is low.

4. Direct pulse compression and self-steepening

Accurate modeling of PSTWM must include the dispersion and SPM. In the following calculations the dispersion is explicitly included by advancing the phase of the signal and pump frequency component in each step of numeric integration. Similarly, SPM is included and applied in the temporal domain. A common known effect of the group velocity mismatch (GVM) in conjunction with three-wave interactions is the reduction of the effective interaction length, the corresponding efficiency, and lengthening of pulse duration. For example, GVM has been pointed out as an obstacle for $\chi^{(2)}$-based compressors for generation of few-cycle pulses [22, 23]. In contrast to those prior findings, it is demonstrated here that in the case of PSTWM, GVM can play a constructive role and enable direct pulse compression or pulse steep-

#128208 - $15.00 USD Received 10 May 2010; revised 1 Jul 2010; accepted 9 Aug 2010; published 13 Aug 2010

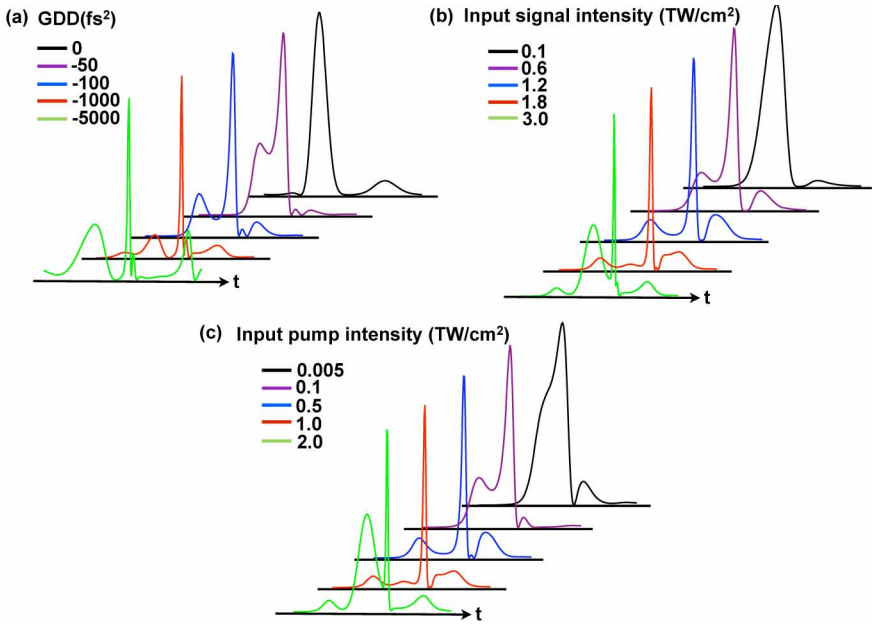

Fig. 5. Signal pulse profiles variations due to (a) input signal phase variations (input signal intensity: 1.6 TW/cm^2; input pump intensity: 0.8 TW/cm^2; input pump phase: flat); (b) input signal intensity variations (input pump intensity: 0.8 TW/cm^2; input signal GDD: $\phi^{(2)} = -401$ fs^2); input pump phase: flat); (c) input pump intensity variations (input signal intensity: 1.6 TW/cm^2; input signal GDD: $\phi^{(2)} = -401$ fs^2); input pump phase: flat).

ening without the need for subsequent compensation of the residual phase.

The case of direct pulse compression by the use of PSTWM is discussed first. In this calculation we choose the crystal length of 265 μm and peak intensities of 1.6 TW/cm^2 for the incident signal pulse and 0.8 TW/cm^2 for the pump pulse. The chosen incident GDD is quadratic, with $\phi^{(2)} = -401$ fs^2, and we first exclude the effect of SPM by setting $n_2^{NL} = 0$. Results of this analysis are shown in Fig. 4.

The slightly chirped signal pulse of $\sim$ 100 fs pulse duration is compressed to 6 fs after PSTWM. Pulse compression process [Fig. 4(d) (Media 3)] is achieved as the signal temporally drifts away from the pump due to the difference in group velocity for signal and pump wavelength. The leading edge of the signal is first depleted, and then the trailing edge of the pulse is depleted. Compression is the aggregate effect of the interplay of three processes. Firstly, temporal phase amplification generates additional bandwidth. Secondly, phase sensitivity of the process results in temporally varying rates of frequency conversion with characteristic length shorter than the pulse durations of driving pulses. Finally, the GVM assists the compression by drifting the pulse envelope and modulating the rate of phase amplification. With a thinner crystal length of 120 μm and a higher intensity of 4 TW/cm^2 for all three waves, which approaches the damage threshold of BBO, it is predicted that a significant pulse compression can be achieved, possibly approaching the single-cycle regime. Further exploration of the parameter space reveals a potential for achieving compressed pulse durations near 6 fs in BBO with the input intensity $>$ 0.2 TW/cm^2 by varying crystal length between 100 μm and 500 μm. We note that the model used in this analysis relies on the usual slowly varying envelope approximation, which is inappropriate for pulse durations approaching a single cycle. Thus while the present analysis predicts significant pulse compression potential, a more refined model will be needed

#128208 - $15.00 USD Received 10 May 2010; revised 1 Jul 2010; accepted 9 Aug 2010; published 13 Aug 2010

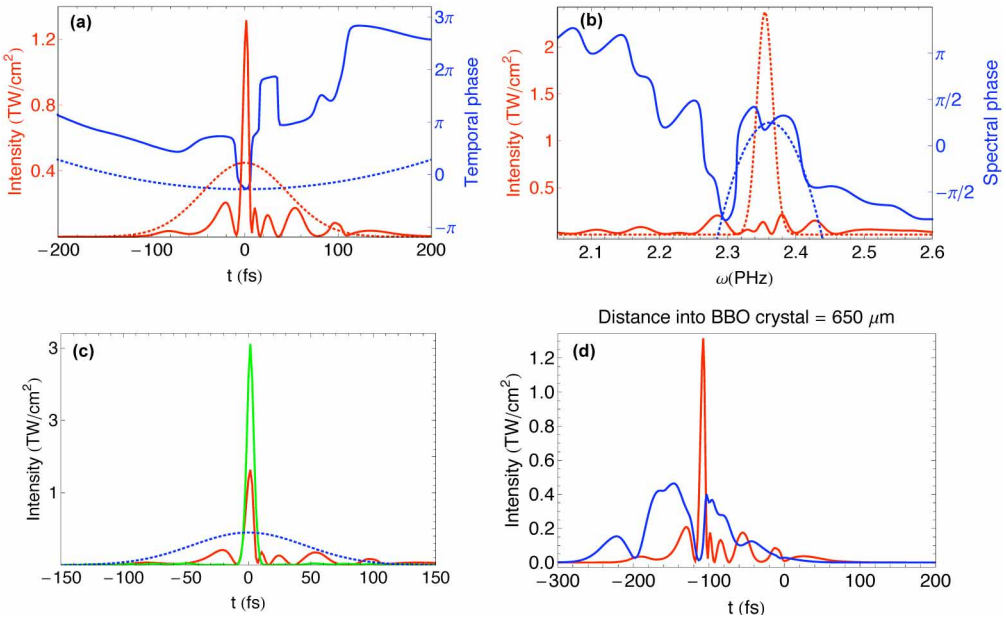

Fig. 6. Pulse compression with SPM in the quadratic case (a) Temporal intensity and phase of signal before (dashed, $\sim$ 100 fs) and after (solid, 6 fs) PSTWM; (b) Spectral intensity and phase of signal before (dashed) and after (solid) PSTWM; (c) Temporal intensity of signal before (blue) and after (red, 6 fs) PSTWM and output with an ideal phase compensation (green, 6 fs); (d) Pulse compression process as signal (red) and pump (blue) traverse BBO (Media 4).

to address the true potential of this technique in the regime of near-single-cycle pulse durations. With an ideal phase compensation of the signal following PSTWM [Fig. 4(c)] it is possible to further improve the contrast and peak power of the produced ultrashort pulse, albeit without further reduction in pulse duration.

To summarize the effect of the varying input GDD, input signal intensity, and input pump intensity on the shape of the signal, each parameter is varied individually (Fig. 5).

It is shown that all three quantities affect the resulting signal pulse shape, which indicates that a careful control of the input parameters is needed to produce desired pulse shapes. In practice, this control amounts to the choice of the type and length of the nonlinear medium and incident pulse amplitude and phase profile.

Now we turn our attention to the inclusion of SPM in the model. Even though n_2^{NL} is small ($n_2^{NL} \approx 5 \times 10^{-16}$ cm^2/W [12]), the resulting SPM could produce a sufficiently large perturbation to the phase-sensitive condition, thus distorting the temporal phase amplification. For example, the predicted nonlinear phase accumulation due to the Kerr effect (B-integral) associated with the intensity of 0.4 TW/cm^2 and BBO crystal length of 650 μm is ~ 1, which can modify the phase relationship between the signal and pump in the PSTWM process. To the first order, the temporal phase amplification gain coefficient is proportional to the product of $\sqrt{I}$ and crystal length L, while the nonlinear phase due to SPM is proportional to $I \times L$, where I is the pulse intensity. Thus the impact of SPM can be minimized by using a lower input intensity compensated by a relatively long crystal length, limited by the GVM-induced pulse walk-off. Considering that this approach to pulse compression relies on a relatively large nonlinear drive and short interaction length, a tradeoff exists between the choice of the input intensity and the

#128208 - $15.00 USD Received 10 May 2010; revised 1 Jul 2010; accepted 9 Aug 2010; published 13 Aug 2010

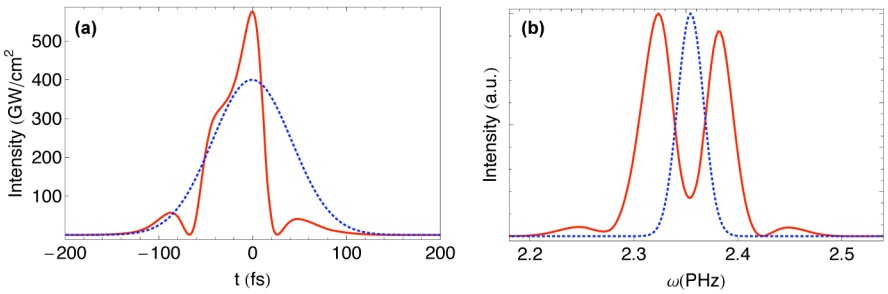

Fig. 7. Production of a steep pulse edge by PSTWM in a 315 μm-long BBO crystal with the signal intensity of 0.4 TW/cm^2 and the pump intensity of 0.2 TW/cm^2: (a) temporal profiles of signal before (dashed) and after (solid) PSTWM; (b) spectrums of signal before (dashed) and after (solid) PSTWM. Peak signal intensities in (b) have been normalized to the initial peak signal intensity.

crystal length. We find that by delaying the pump pulse by 45 fs and choosing an input intensity of 0.45 TW/cm^2 for the signal and 0.2 TW/cm^2 for the pump with $\phi^{(2)} = -657$ fs^2 for both the signal and the pump, it is predicted that the signal pulse can still be compressed from ~ 100 fs to near 6 fs in a crystal length of 650 μm, as shown in Fig. 6.

Similar to the SPM-free compression case, an ideal spectral phase compensation of the output signal improves the pulse contrast, but does not shorten the pulse duration [Fig. 6(c)]. It is also noted that while this method leads to a relatively low conversion efficiency, the recompressed pulse peak power is still somewhat greater than that of the incident pulse, despite the method of compression which involves the power deamplification as one of the mechanisms.

An additional potentially useful pulse shape can be obtained by terminating the described compression process (shortening the crystal length) before a significant compression has occurred. In the process of pulse compression driven by PSTWM and GVM, depletion of one edge of the pulse is induced for shorter interaction length, before a significant temporal walk-off of two pulse envelopes has occurred. When one edge of the signal is depleted, self-steepening occurs, as shown in Fig. 7. The magnitude of this self-steepening can be controlled by varying the interaction length. Such self-steepening produces pulse rise times significantly shorter than the transform-limited pulse duration of the original pulse, leading to potentially beneficial applications in laser-matter interactions requiring fast pulse rise times.

5. Production of pulse doublets and pulse trains

Various configurations of PSTWM have been discussed, where signal or its rise time can be shaped to produce features shorter than that allowed by the initial transform-limited bandwidth. Now we turn attention to the features of the modification of the pump pulse involved in the PSTWM process. With dispersion and SPM included, it is found that femtosecond pulse doublets and closely spaced pulse trains can be produced at the pump wavelength. Pulse doublets and pulse trains have numerous practical applications. Pulse doublets could be used in applications such as collinear pump-probe studies, spectral phase interferometry for direct electric-field reconstruction (SPIDER) [24], and coherent quantum control [25], while pulse trains can also be applied to coherent control [26, 27], as well as tunable THz electromagnetic wave generation [28] and quasi-phase-matching of high-harmonic generation [29]. Several methods have been demonstrated for generating pulse doublets and pulse trains, including multicrystal birefringent arrangements [30], phase manipulation [31], and phase-matched difference-frequency mixing [32]. In all of these methods the resulting pulse train contains pulses exhibiting pulse

#128208 - $15.00 USD Received 10 May 2010; revised 1 Jul 2010; accepted 9 Aug 2010; published 13 Aug 2010

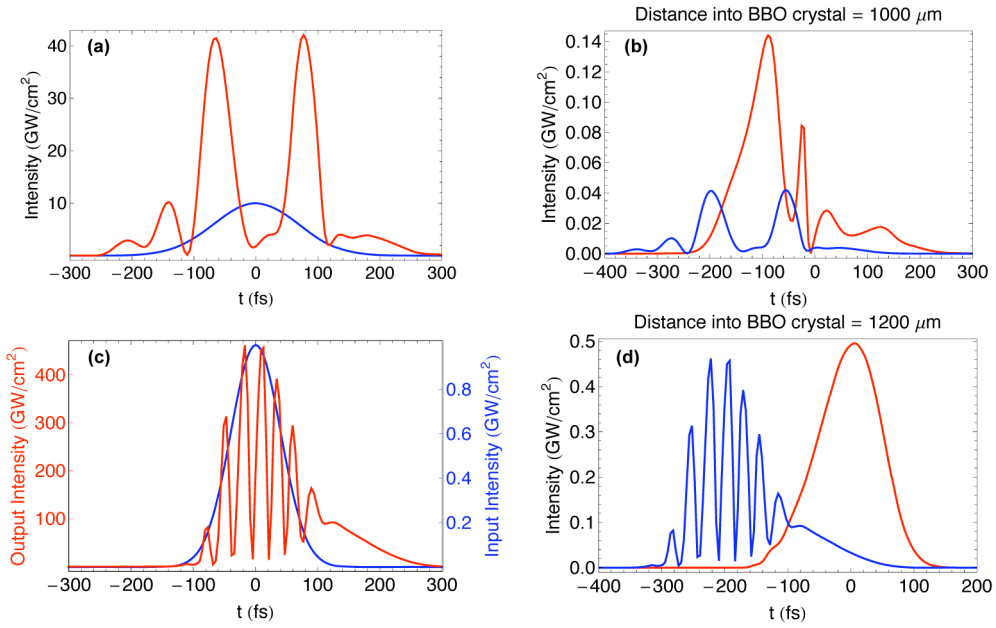

Fig. 8. Generation of pulse doublets and pulse trains at the pump frequency. Production of pulse doublets: (a)temporal profile of pump before (blue) and after PSTWM (red); (b) Pulse doublets shaping process as pump (blue) and signal (red) go through BBO (Media 5). Production of pulse trains: (c) temporal profile of pump before (blue) and after PSTWM (red); (d) Pulse trains shaping process as pump (blue) and signal (red) go through BBO (Media 6).

durations identical or longer than the transform-limited incident pulse. In contrast, PSTWM can produce pulse doublets and pulse trains where individual pulses are shorter than the duration of the original driving pulse, and with total pulse train duration on the order of the original driving pulse.

During the PSTWM process, energy is periodically converted between the signal and the pump as the signal drifts from the pump due to GVM. In Fig. 8(a), production of a pulse doublet is demonstrated by the use of crystal length of 1 mm. In this example the initial temporal phases of the signal and the pump are both quadratic ($\phi^{(2)} = -2689$ fs^2 for signal and $\phi^{(2)} = 2176$ fs^2 for pump), and the initial signal and pump peak intensities are 100 GW/cm^2 and 10 GW/cm^2, respectively. It can be seen that the pulse doublet produced has peak intensity about 40 GW/cm^2. In Fig. 8(b), the pulse train is shaped using a linear phase as previously discussed in Fig. 3(b), with BBO crystal length of 1.2 mm and the initial signal and pump peak intensities of 1 TW/cm^2 and 1 GW/cm^2, respectively. Here, the pulse train with peak intensity of $\sim$450 GW/cm^2 is produced at the pump frequency. Thus introducing the signal at high energy relative to that of the pump can result in high-energy pulse doublets and pulse trains at the pump frequency. At the fixed GDD, the relative spacing between the pulses in the pulse train can be controlled by adjusting the relative linear excess phase of the signal pulse.

6. Conclusion

In conclusion, a novel method of direct temporal pulse shaping via temporal phase amplification has been proposed and analyzed. While the method fundamentally relies on the process of PSTWM, significant benefits in ultrafast pulse shaping are derived with the assistance of GVM.

#128208 - $15.00 USD Received 10 May 2010; revised 1 Jul 2010; accepted 9 Aug 2010; published 13 Aug 2010

The proposed implementation of the method is in a degenerate and collinear configuration, where pump pulses can be readily produced from the same source. Our analysis indicates that the simple quadratic variation of temporal phase facilitates pulse compression and self-steeping, with features significantly shorter than the transform-limited original pulse. Thus PSTWM can act as a direct pulse compressor based on the intertwined effect of phase amplification and GVM, even without the subsequent phase compensation. Furthermore, it has been shown that pulse doublets and pulse trains can be produced at the pump frequency by utilizing residual linear phase in the signal.

Since the PSTWM is sensitive to both pulse amplitude and phase and can be tuned by adjusting the time-varying phase of one or both of the incident pulses, considerably more control is available than in other nonlinear pulse shaping methods demonstrated to date. Phase sensitivity mandates the use of a single source to produce both the signal and the pump pulses for robust practical applications, with the simplest implementation in a degenerate, collinear configuration described at length in this work.

Acknowledgements

This work has been supported in part by the Defense Advanced Research Projects Agency (DARPA), Contract HR0011-08-1-0066.

#128208 - $15.00 USD Received 10 May 2010; revised 1 Jul 2010; accepted 9 Aug 2010; published 13 Aug 2010